Design, Synthesis, and In-silico Evaluation of Benzyl oxybenzoate Derivatives as Dual HDAC Inhibitors for Cancer and CNS Disorders

Dhiaa Ali Abdulkader*, Monther F. Mahdi*

Department of Pharmaceutical Chemistry, College of Pharmacy, Mustansiriyah University, Baghdad-Iraq.

Article Info:

Received 28 Apr 2025
Revised 5 May 2025
Accepted 26 May 2025
Published 31 Dec 2025
Corresponding Author email:
dr.monther.f71@uomustansiriyah.edu.iq
Orcid: https://orcid.org/0000-0002-2069-4121

DOI: https://doi.org/10.32947/ajps.v25i5.1307

Abstract:

Histone deacetylase (HDAC) inhibitors have garnered attention as possible therapies for disorders affecting the central nervous system (CNS) and cancer. Because HDACs, particularly HDAC1 and HDAC2, are overexpressed in many cancers and govern neurological diseases, they are dual targets for therapeutic interventions.

Therefore, this study aims to synthesize benzyl oxybenzoate and use pharmacokinetic analyses and molecular docking to evaluate their potential as HDAC inhibitors.

After synthesizing benzoyl oxybenzoate derivatives, their potential as HDAC inhibitors was evaluated by comparing their binding affinity and mechanism to that of SAHA, a well-known HDAC inhibitor, utilizing molecular docking against HDAC2. To forecast pharmacokinetics, the ADME profiles of these substances—such as oral bioavailability and blood-brain barrier (BBB) permeability—were also assessed.

A number of synthetic compounds showed promising binding affinities against HDAC2, indicating their potential as HDAC inhibitors. According to the results, the designed compounds that were found may be investigated further as dual-action medications for CNS diseases and cancer.

Keywords: HDAC inhibitors; Benzyl oxybenzoate derivatives; Molecular docking; Cancer; CNS disorders.

تصميم، تخليق، والتقييم الحاسوبي لمشتقات بنزويل أوكسي بنزوات

ضياء علي عبد القادر*, منذر فيصل مهدي

قسم الكيمياء الصيدلانية، كلية الصيدلة، جامعة المستنصرية، بغداد، العراق

الخلاصة:

لقد حظيت مثبطات الهيستون ديستيليز باهتمام متزايد باعتبارها علاجات محتملة لاضطرابات الجهاز العصبي المركزي والسرطان. ونظرا لكون انزيمات الهستون ديستيليز ولا سيما واحد واثنان بانها مفرطة الفعالية في الكثير من انواع السرطان وتتحكم في امراض عصبية متنوعة، فانها تعد اهداف مزدوجة للادوية العلاجية.

وعليه يهدف هذا البحث الى تصنيع مشتقات من مركب بنزيل اوكسي بنزوات، واستخدام تحليلات الدواء الحركية والارتساء الجزيئي لمعرفة امكانياتها كمثبطات للهستون ديستيليز.

وبعد صنع مشتقات البنزيل اوكسي بنزوات فقد تم مقارنة فعالية المشتقات ومعرفة قوة ارتباطها والية عملها كمثبط للهستون ديستيليز مع المثبط المعروف بالساها وذلك باستخدام تقنية الارتساء الجزيئي مع الهستون ديستسليز ٢, وكذلك تقييم التوافر الحيوي الفموي ونفاذية الحاجز الدموي الدماغي لمعرفة امكانية المشتقات العلاجية.

وقد اظهرت المشتقات قدرة ارتباط جيدة مع الهستون ديستسليز ٢ مما يشير الى امكانية استخدامها كمثبطات فعالة للهستون ديستيليز. وتشير النتائج الى ان المركبات المصنعة قد تكون جديرة بمزيد من الدراسة والتطوير كادوية مزدوجة الفعالية لعلاج امراض السرطان والجهاز العصبي المركزي.

الكلمات المفتاحية: مثبطات الهستون ديستيلز, مشتقات بنزيل اوكسي بنزوات، الارتساء الجزيئي، السرطان، اضطرابات الجهاز العصبي المركزي.

Introduction

To date, the majority of the medications utilized to treat cancer patients are cytotoxic medicines. Although there has been significant success in treating patients with these substances, this progress has halted, and alternative strategies will be required to keep improving patient care. Current chemotherapy treatments target the proliferation and differentiation abnormalities found in many cancer forms. (1)

The deacetylation of lysine residues on the N-terminal tails of histone proteins is catalyzed by a class of enzymes known as histone deacetylases (HDACs). as depicted in Figure 1. There are four different classes of HDACs. The selected targets, HDAC1 and HDAC2, are class 1 enzymes that change chromatin and are believed to be implicated in the development of cancer. (2)

Particularly, HDACs 1 and 2 are overexpressed in human malignancies, and in some cellular situations, suppression increases apoptosis. They have 82% sequence identity and 92% sequence homology in common. Furthermore, new preclinical research points to HDACs' involvement in neurodegenerative and inflammatory illnesses. (3)

Surprisingly, it appears that blocking a shared set of targets or pathways may occasionally result in therapeutic advantages for a variety of CNS disorders. Histone deacetylases (HDACs) are a superfamily of enzymes that have been identified as a significant therapeutic target for a variety of human illnesses, initially for the treatment of cancer. On the other hand, HDAC-based therapies have another significant use: they may be used to treat human central nervous system problems. (4)

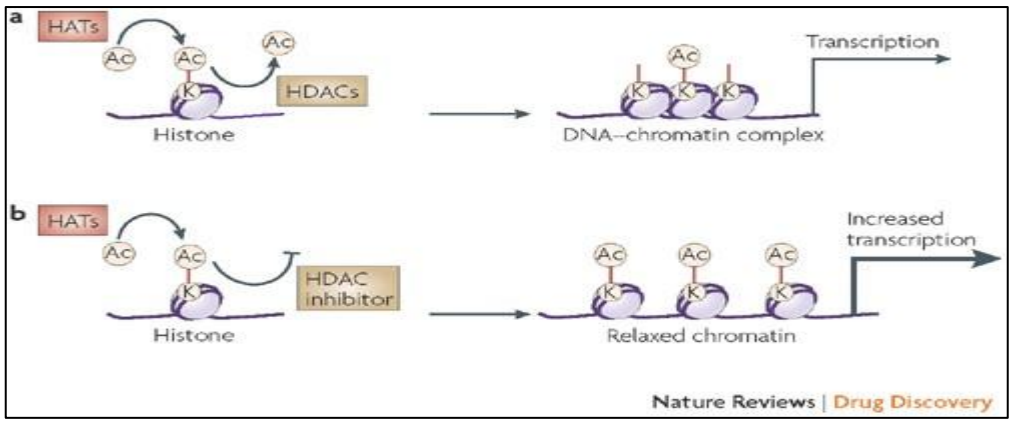

Figure 1: HDAC inhibitors' impact on transcription and chromatin remodeling (4)

Reducing histone acetylation levels and making proteins more compact by removing acetyl groups is the work of histone deacetylases (HDACs). This process limits gene transcription. As a possible strategy for promoting functional recovery after a stroke, HDAC inhibitors boost chromatin transcriptional activity, which in turn increases the expression of several genes associated with neuroplasticity. (5)

Irregular histone acetylation can be linked to many neurological disorders. Rubinstein-Taybi Syndrome (RTS) is a highly uncommon genetic condition in humans resulting from mutations in the histone acetyltransferase (HAT) domain of the CREB-binding protein (CBP) gene. This loss-of-function mutation induces hypoacetylation in transgenic mice, analogous to cognitive abnormalities observed in humans. Studies in mice have demonstrated that SAHA, a non-selective Class I, IIb HDAC inhibitor, can rectify hypoacetylation in the brain and the associated cognitive deficits. This discovery offers encouraging data for possible therapeutic alternatives. (6)

On the other hand, research has shown that HDAC inhibitors can protect neurones from damage and that HDAC expression alters after CNS injury. One study found that HDAC2 negatively affects synaptic plasticity in animal's models of neurodegeneration. (7)
Researchers have shown that the mRNA and protein expression of HDAC1, 2, and 5 was altered in patients having major depressive illness, schizophrenia, and bipolar disorder when they examined their brains after death. Because it selectively inhibits all class I HDACs, valproate is a common medicine for the treatment of bipolar disorder. Bipolar disorder is often treated with lithium medication in addition to the standard antipsychotic and as a companion to antidepressants. In addition, HDAC2 is known to have a major role in controlling the response to atypical antipsychotics. (8)
Systemic muscle atrophy results from the degradation of α-motor neurones in the anterior horn of the spinal cord, a neuromuscular disorder which is called spinal muscular atrophy in children. (9)
Butyrate, valproate, phenyl-butyrate, and vorinostat are among the class I and II HDAC inhibitors that have been shown to effectively increase SMN2 expression in SMA patient fibroblasts. (10)
Since all neurons depend on axonal transport, modifying tubulin acetylation may be a strategy for treating further nervous system problems. For example, it has been demonstrated that the HDAC6-specific inhibitor tubastatin A restores mitochondrial axonal transport in primary hippocampus neurons exposed to neurotoxicity in Alzheimer's disease (AD). (11)
In both cellular and fly models of Parkinson's disease (PD), broad HDAC inhibitors prevent α-synuclein-dependent cytotoxicity. (12) In this case, an improvement in axonal transport brought about by HDAC6 inhibition probably contributes to the positive benefits of HDAC to the positive benefits of HDAC inhibition previously mentioned in polyglutamine disorder. (13)

MATERIALS AND METHODS

Every chemical and solvent were bought commercially by Merck or Sigma-Aldrich. The KBr/Shimadzu spectrophotometer was used to measure the infrared spectra. The 500 MHz Bruker spectrometer was used to measure the 1H-NMR and 13C-NMR spectra. An electro-thermal melting point device was used to determine the melting points without making any adjustments.

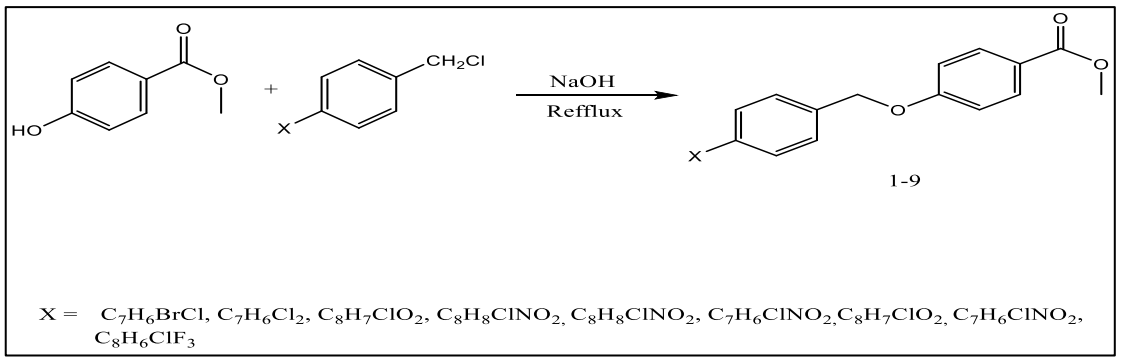

Scheme 1. Synthesis of benzyl oxybenzoate derivatives

In a conical flask, methyl paraben (0.304 gm, 2 mmol) was gradually added to NaOH (0.08 gm, 2 mmol) that had been dissolved in 8 mL of methanol. The mixture was then stirred for 40 minutes at room temperature. After two hours of reflux, 2 mmol of benzoyl chloride derivatives will be added drop by drop to the parabens that are dissolving. The products are then obtained by cooling, filtering the precipitate, washing it with water, and recrystallizing it with methanol.

Compound 1: Methyl 4-((4-bromobenzyl) oxy) benzoate, white powder m.p: 188°C-190°C. FTIR (KBr) 3104cm^{-1}, 3072 cm-^{1} (C-H aromatic), 2999, 2948 cm^{-1} (C-H alkane), 1704 cm^{-1} (C=O ester), 1604, 1427 cm^{-1} (C=C aromatic), 1258 cm^{-1} (C-O ester), 1164 cm^{-1} (C-O aromatic ether), 850 cm^{-1} (para substitution).

1H-NMR-DMSO d6, 8.19-7.47 ppm (multiplet, 8H) aromatic ring, 4.91 ppm (singlet, 2H) CH2-O (ether), 3.90 ppm (singlet, 3H) CH3-O ester.

13C-NMR-DMSO d6, 166.29 (C=O ester), 162.46 (=C-O), 136.38-115.30 (carbon of aromatic ring), 69.14 (C-O of ether), 52.32 (CH3-O of ester)

Compound 2: Methyl 4-((4-chlorobenzyl) oxy) benzoate, white powder m.p: 154°C-156°C.

FTIR (KBr) 3106 cm^{-1} (C-H aromatic), 2986, 2941 cm^{-1}(C-H alkane), 1701 cm^{-1} (C=O ester), 1599, 1420 cm^{-1} (C=C aromatic), 1247 cm^{-1} (C-O ester), 1177 cm^{-1} (C-O aromatic ether), 843 cm^{-1} (para substitution).

1H-NMR-DMSO d6, 7.97-6.48 ppm (multiplet, 8H) aromatic ring, 5.20 ppm (singlet, 3H) CH2-O (ether), 3.82 ppm (singlet, 3H) CH3-O ester.

13C-NMR-DMSO d6, 166.28 (C=O ester), 162.35 (=C-O), 141.78-115.27 (carbon of aromatic ring), 69.02 (C-O of ether), 52.28 (CH3-O of ester).

Compound 3: 3-((4-(methoxycarbonyl)phenoxy)methyl)benzoic acid, white powder m.p: 301°C-303°C. FTIR (KBr) 3580, 3468, 3310, 3292, 3264 cm^{-1} (O-H carboxyl), 2975 cm^{-1} (C-H aromatic), 2902 cm^{-1} (C-H alkane), 1709 cm^{-1} (C=O carboxyl), 1691 cm^{-1} (C=O ester), 1599, 1501 cm^{-1} (C=C aromatic), 1253 cm^{-1} (C-O of substituted ester), 1190 cm^{-1} (C-O ester), 1162 cm^{-1} (C-O aromatic ether), 890 cm^{-1} (para substitution).

1H-NMR-DMSO d6, 10.38 ppm (singlet, 1H) carboxyl, 7.86-6.56 ppm (multiplet, 8H) aromatic ring, 3.81 ppm (singlet, 3H) CH2-O (ether), 3.66 (singlet, 3H) CH3-O ester.

13C-NMR-DMSO d6, 172.52 (C=O carboxyl), 166.53 (C=O ester), 162.44 (=C-O), 155.66-115.22 (carbon of aromatic ring), 68.04 (C-O of ether), 52.09 (CH3-O of ester).

Compound 4: Methyl 4-((2-methyl-3-nitrobenzyl) oxy) benzoate, pale yellow powder m.p: 176°C-178°C. FTIR (KBr) 3095 cm^{-1}(C-H aromatic), 2952, 2904 cm^{-1} (C-H alkane), 1703 cm^{-1} (C=O ester), 1604, 1489 cm^{-1} (C=C aromatic), 1512, 1317 cm^{-1} (NO2), 1266 cm^{-1} (C-O ester), 1183 cm^{-1} (C-O aromatic ether), 850 cm^{-1} (para substitution).

1H-NMR-DMSO d6, 8.33-6.86 ppm (multiplet, 7H) aromatic ring, 5.40 ppm (singlet, 3H) CH2-O (ether), 3.80 ppm (singlet, 2H) CH3-O ester, 2.10 ppm (singlet, 3H) CH3.

13C-NMR-DMSO d6, 166.28 (C=O ester), 162.35 (=C-O), 141-115 (carbon of aromatic ring), 69 (C-O of ether), 52.28 (CH3-O ester), 51.28 (CH3).

Compound 5: Methyl 4-((4-methyl-3-nitrobenzyl) oxy) benzoate, pale yellow powder m.p: 168°C-170°C. FTIR (KBr, cm^{-1}) 2984 cm^{-1} (C-H aromatic), 2960, 2904 cm^{-1} (C-H aliphatic), 1702 cm^{-1} (C=O ester), 1602, 1486 cm^{-1} (C=C aromatic), 1511, 1317 cm^{-1} (NO2), 1266 cm^{-1} (C-O ester), 1160 cm^{-1} (C-O aromatic ether), 847 cm^{-1} (para substitution).

1H-NMR-DMSO d6, 8.00-7.15 ppm (multiplet, 7H) aromatic ring, 5.33 ppm (singlet, 3H) CH3-O (ester), 3.83 ppm (singlet, 2H) CH2-O ether, 2.45 ppm (singlet, 3H) CH3.

13C-NMR-DMSO d6, 166.26 (C=O ester), 162.22 (=C-O), 147-115 (carbon of aromatic ring), 68.74 (C-O of ether), 52.34 (CH3-O ester), 22.43 (CH3).

Compound 6: Methyl 4-((3-nitrobenzyl) oxy) benzoate, pale yellow powder m.p: 161°C-163°C.

FTIR (KBr, cm−1) 3072 cm^{-1} (C-H aromatic), 2980, 2900 cm^{-1} (C-H aliphatic), 1702cm^{-1} (C=O ester), 1604, 1434 cm^{-1} (C=C aromatic), 1527, 1311 cm^{-1} (NO2), 1282 cm^{-1} (C-O ester), 1156 cm^{-1} (C-O aromatic ether), 844 cm^{-1} (para substitution).

1H-NMR-DMSO d6, 8.30-6.88 ppm (multiplet, 8H) aromatic ring, 5.39 ppm (singlet, 2H) CH2-O (ether), 3.83 ppm (singlet, 3H) CH2-O ester.

13C-NMR-DMSO d6, 166.53 (C=O ester), 162.54 (=C-O), 135-115 (carbon of aromatic ring), 69.10 (C-O of ether), 52.27 (CH3-O ester).

Compound 7: 4-((4-(methoxycarbonyl)phenoxy)methyl)benzoic acid, white powder m.p: 298°C-300°C. FTIR (KBr, cm^{-1}) 3387, 3206, 3196 cm^{-1} (O-H carboxyl), 2966 cm^{-1} (C-H aromatic), 2905 cm^{-1} (C-H aliphatic), 1704 cm^{-1} (C=O carboxyl), 1604 cm^{-1} (C=O ester), 1513, 1427 cm^{-1} (C=C aromatic), 1255 cm^{-1} (C-O of substituted ester), 1162 cm^{-1} (C-O ester), 1108 cm^{-1} (C-O aromatic ether), 846 cm^{-1} (para substitution).

1H-NMR-DMSO d6, 10.51 ppm (singlet, 1H) carboxyl, 7.95-6.88 ppm (multiplet, 8H) aromatic ring, 5.19 ppm (singlet, 2H) CH2-O (ether), 3.46 (singlet, 3H) CH3-O ester.

13C-NMR-DMSO d6, 167.67 (C=O carboxyl), 166.52, 166.29, 165.76 (C=O ester), 162.53 (=C-O), 137.84-115.29 (carbon of aromatic ring), 69.25 (C-O of ether), 52.31, 52.08 (CH3-O of ester).

Compound 8: Methyl 4-((4-nitrobenzyl) oxy) benzoate, pale yellow powder m.p: 160°C-162°C.

FTIR (KBr, cm^{-1}) 2971 cm^{-1} (C-H aromatic), 2903 cm^{-1} (C-H aliphatic), 1721 cm^{-1} (C=O ester), 1596, 1405 cm^{-1} (C=C aromatic), 1537, 1313 cm^{-1} (NO2), 1251 cm^{-1} (C-O ester), 1164 cm^{-1} (C-O aromatic ether), 837 cm^{-1} (para substitution).

1H-NMR-DMSO d6, 8.03-7.00 ppm (multiplet, 8H) aromatic ring, 5.18 ppm (singlet, 2H) CH2-O (ether), 3.82 ppm (singlet, 3H) CH3-O ester.

13C-NMR-DMSO d6, 166.30 (C=O ester), 162.48 (=C-O), 135-115 (carbon of aromatic ring), 69.11 (C-O of ether), 52.31 (CH3-O ester).

Compound 9: Methyl 4-((4-(trifluoromethyl) benzyl) oxy) benzoate, white powder m.p: 144°C-146°C. FTIR (KBr, cm−1) 3055 cm-1 (=CH aromatic), 2972, 2895 cm-1 (-CH alkane), 1717 cm-1 (C=O ester), 1593, 1447 cm-1 (C=C aromatic), 1271 cm-1 (C-O ester), 1194 cm-1 C-O aromatic ether), 906 cm-1 (para substitution).

1H-NMR-DMSO d6, 7.99-6.27 ppm (multiplet, 7H) aromatic ring, 5.19 ppm (singlet, 2H) CH2-O (ether), 3.83 ppm (singlet, 3H) CH3-O ester.

13C-NMR-DMSO d6, 166.01 (C=O ester), 164.25 (=C-O), 154-122 (carbon of aromatic ring), 65.01 (C-O of ether), 45.60 (CH3-O ester).

Molecular docking study

1. Protein receptor and ligand preparation

- ✓ The Protein Data Bank (PDB) provided the crystal structure of an HDAC homolog complexed with SAHA (PDB code: 1C3S). Water molecules were eliminated and hydrogen atoms were added to achieve amino acid residues and the proper ionization tautomeric states in the target protein structures.
- ✓ The structures of the ligand molecules are drawn using ChemDraw (version 22.0.022).
- ✓ To reduce the twelve selected ligand molecules' energy, a molecular mechanics' force field was implemented in Chem3D (version 22.0.022).

2.The molecular docking method

The Genetic Optimisation for Ligand Docking (GOLD) tool at the Cambridge Crystallographic Data Centre (CCDC) was employed in the molecular docking methodology. A software application developed in Cambridge, ChemDraw, was likewise employed. This study was performed utilising version 2022.3.0. The GOLD suite's Hermes visualiser (version 2022.3.0, Cambridge, England) was utilised to prepare the receptor for docking and capture images. The binding location comprises all protein residues in the downloaded protein structure complexes that are within 10 Å of the reference ligands. The early termination option was disabled, the highest-ranked solution was set as the default, and the quantity of generated poses was restricted to 10. The setting instructions pertained to Chemscore Kinase. The piecewise linear potential (ChemPLP) serves

as a scoring function. The outcomes were subsequently archived as mol.2 files. (14) ChemBioOffice, (version 22.0.022), was used to display the chemical structures of the ligands.

Several different HDACs (7ZZP, 1C3S, and 7JVU) were obtained from the PDB database to carry out ensemble docking. Because it exhibits an interaction with SAHA, the HDAC crystal structure 1C3S was chosen.

We examined docking data to understand the interactions between the ligands we synthesized and the amino acid residues of the HDACs protein. The impacts of docking position, binding free energy, and binding mode were taken into account in this investigation.

3.ADME procedure

The Swiss ADME server was used to assess the pharmacokinetic profile of our drugs, including their bioavailability, affinity for P-gp, and BBB (blood-brain barrier) permeability. Excluding compounds with insufficient ADME (absorption, distribution, metabolism, and excretion) properties is an essential step in identifying therapeutic candidates that show the best safety and promise for oral administration. These compounds are likely to fail during later stages of drug development (15). The SwissADME program was used to export the ligands as SMILE names after they were first produced using the ChemDraw software.

Results and Discussion

In- The binding mechanisms of many active drugs can be well understood using molecular docking. (16-18). In this study, nine novel compounds and one FDA-approved medication (SAHA) were tested against the HDAC-2 receptor using molecular docking.

The results showed that each compound displayed a similar binding behavior in the HDAC receptor's binding region. As indicated in Table 1, the binding pockets were recognized by their PDB ID, 1C3S. The compounds' docking scores were contrasted with those of the reference ligand, SAHA. According to docking scores, all of the novel compounds are comparable to the reference ligand (SAHA), suggesting good binding.

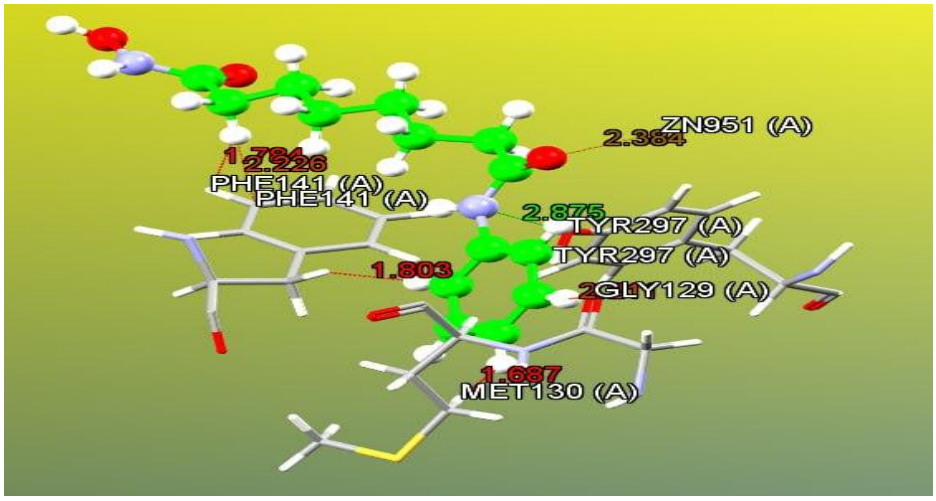

Figure (2). 3D ligand interaction of SAHA with HDAC-2.

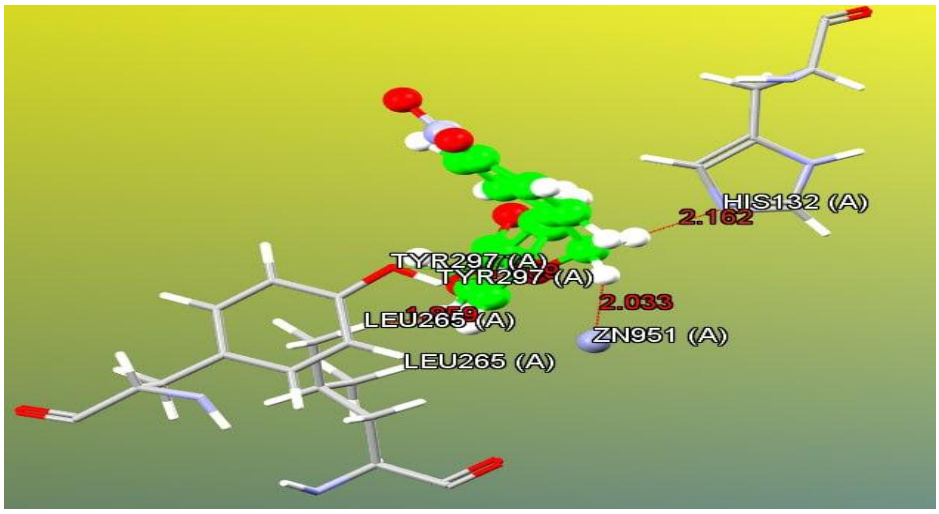

Figure (3). 3D ligand interaction of compound 9 with HDAC-2.

The Swiss ADME server has examined the impact of the synthesized analogues on the ADME properties in order to identify the safer and more promising drug candidate or candidates and to weed out compounds that might not pass the following stages of drug manufacture because of unfavorable ADME features. Lipinski's rule of five requires that medications meant for oral administration have a molecular weight beneath 500, a partition coefficient (o/w) below 5, less than five hydrogen bond donors, and fewer than ten hydrogen bond acceptors. A polar surface area of less than 140 Å is also necessary for the medicine because it is directly related to its bioavailability. PSA values and the medication's oral bioavailability are inversely correlated. To increase oral bioavailability, all compounds must passively absorb, which is made easier by having a topological polar surface area (TPSA) of less than 140 Å. (19)

Table (1): The binding energies for the designed compounds and control (SAHA) docked against HDAC-2 receptor.

No.	Molecule structure	PLP Fitness	H-Bond	Short contact
1.	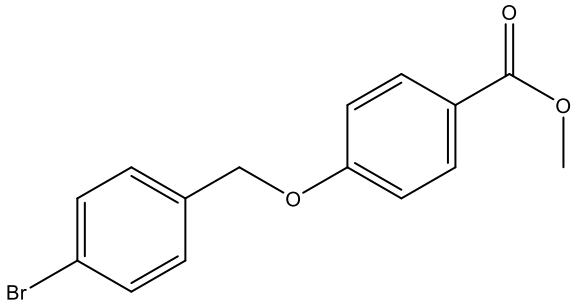	77.60	TYR 297	ZINC, TYR 297, ASP 258, MET 130, LEU 265, GLY 140, HIS 132, PHE 141

2.	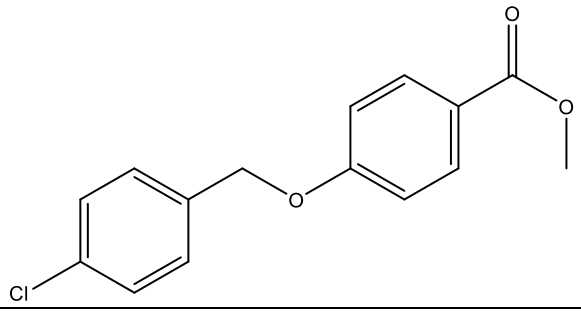	**77.41**	TYR 297	ZINC, TYR 297, ASP 258, LEU 265, MET 130, GLU 92, PHE 141, HIS 132
3.	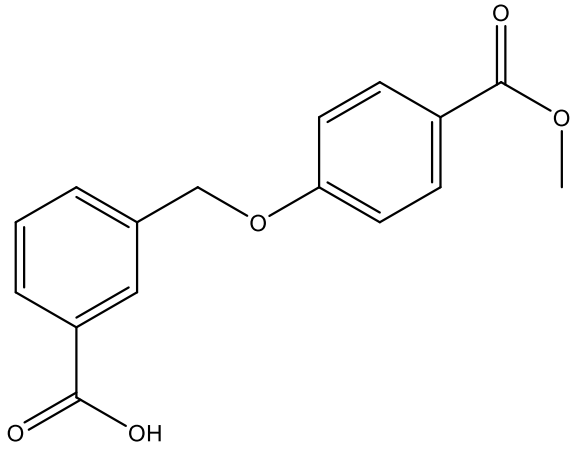	**74.01**	TYR 297, LEU 265, HIS 170, TYR 91, GLN 192, GLU 92	ZINC, TYR 297, ASP 258, LEU 265, TYR 91, PHE 200, GLU 92, PHE 141, GLY 140,
4.	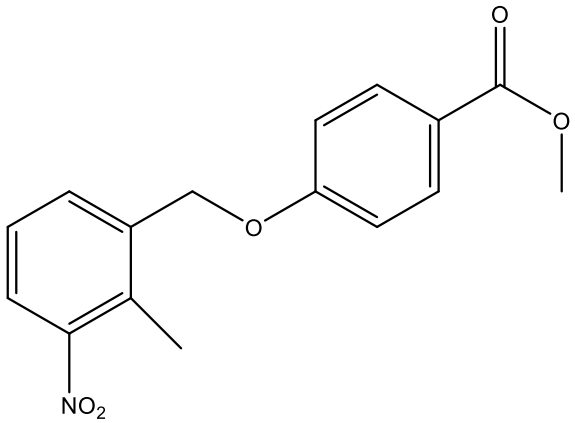	**73.98**	TYR 297, PHE 198	ZINC, TYR 297, ASP 258, TYR 91, PHE 141, PHE 200, GLY 140, GLU 92,
5.	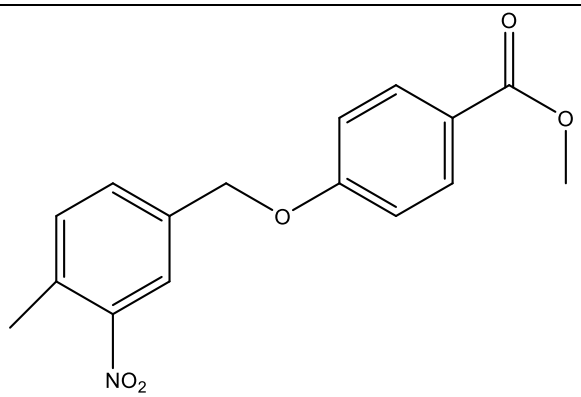	**74.33**	TYR 297	ZINC, PHE 200, ASP 258, LEU 265, TYR 297, GLY 140, GLU 92, HIS 131, GLY 129, MET 130, LEU 23

6.	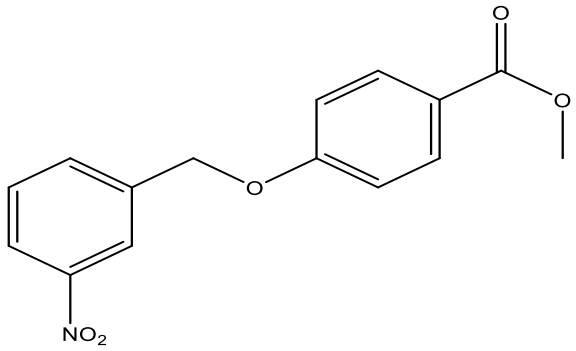	**74.66**	TYR 297	ZINC, LEU 265, TYR 297, ASP 258, HIS 132, GLY 129, TYR 91, LEU 23, HIS 131, GLU 92
7.	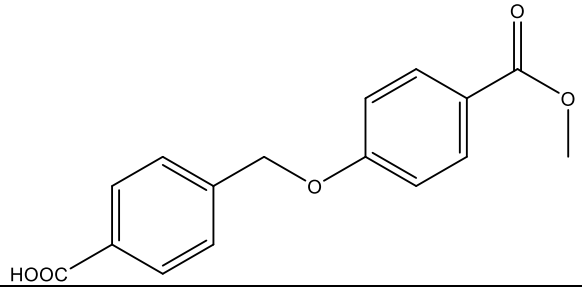	**74.42**	GLY 140, TYR 297, ASP 258	ZINC, GLY 140, HIS 132, TYR 297, ASP 258, LEU 265, TYR 196, LYS 267
8.	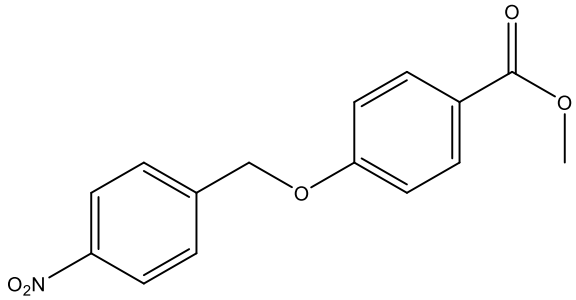	**75.32**	TYR 297	ZINC, ASP 258, TYR 297, LEU 265, HIS 132, LEU 23,
9.	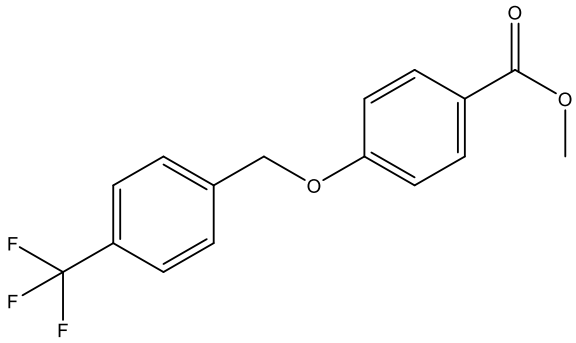	**82.70**	TYR 297	ZINC, LEU 265, ASP 258, LEU 23, HIS 132, TYR 297, GLY 140, MET 130.
SAHA	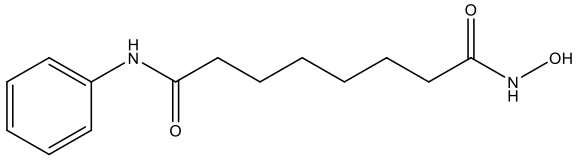	**78.95**	TYR 297, GLN 192, ASP 168, HIS 131, HIS 132, GLU 92, PH2 192, LEU 265, GLY 140	ZINC, HIS 132 PHE 198 HIS 131

Table 2. Insilico ADMET screening for proposed compounds

Compounds	TPSA	Water Solubility	G.I Absorption	BBB Permeability	Lipinski	Veber
1	35.53 Å²	Moderately soluble	High	Yes	Yes	Yes
2	35.53 Å²	Moderately Soluble	High	Yes	Yes	Yes
3	72.83 Å²	Moderately soluble	High	Yes	Yes	Yes
4	81.35 Å²	Moderately Soluble	High	No	Yes	Yes
5	81.35 Å²	Moderately Soluble	High	No	Yes	Yes
6	81.35 Å²	Moderately Soluble	High	No	Yes	Yes
7	72.83 Å²	Moderately Soluble	High	Yes	Yes	Yes
8	81.35 Å²	Moderately Soluble	High	No	Yes	Yes
9	35.53 Å²	Moderately Soluble	High	Yes	Yes	Yes
SAHA	78.43 Å²	Soluble	High	No	Yes	Yes

Discussion

The top nine compounds were selected, and it was found that each one binds to the active sites of the HDAC-2 receptor with a good binding energy. Compound (9) exhibits the strongest H-bonding with amino acids and the highest PLP fitness of 82.70, as indicated in Table (1). The binding energies of compounds 1–8 are all lower than those of the standard medication SAHA, which accounts for the PLP's 77.60, 77.41, 74.01, 73.98, 74.33, 74.66, and 75.32 fitness values, respectively.

According to figure (2), the original ligand SAHA's energy score (PLP fitness) was 78.95. It formed multiple hydrogen bond interactions with the amino acids TYR 297, GLN 192, ASP 168, HIS 131, HIS 132, GLU 92, PH2 192, LEU 265, and GLY 140 in the binding sites, as well as multiple short contacts with HIS 132, PHE 198 and HIS 131 amino acids. Zinc binding also took place with the amide group's carbonyl. This was discovered to recover the SAHA binding mode that was previously described in the HDLP X-ray crystal structure (PDB ID: 1C3S).

With an energy score (PLP fitness of 82.70), the newly synthesized compound 9 had the best binding affinity in figure (3). Compound 9 forms a hydrogen bond interaction with TYR 297 amino acid in the binding site and makes multiple short contacts with LEU 265, ASP 258, LEU 23, HIS 132, TYR 297, GLY 140, and MET 130 amino acids in addition to zinc binding with the carbonyl of the ester group, the binding mode was consistent with SAHA.

All of our compounds complied with Lipinski's guidelines and were able to be absorbed orally due to their primarily moderate molecular weight, as shown in Table 2. Furthermore, every compound aside from 4, 5, 6, and 8 can cross the blood-brain barrier, indicating a central impact. [20].

Conclusion

The synthesized benzyl oxybenzoate derivatives exhibit potent binding interactions with HDAC comparable to the FDA-approved HDAC inhibitor SAHA and have promise as treatment possibilities for both cancer and central nervous system

disorders. Key binding residue alignment was verified by molecular docking, and ADME studies revealed advantageous profiles for BBB penetration. These results imply that derivatives of benzyl oxybenzoate might be useful HDAC inhibitors with uses outside of cancer, especially in neuroprotection. To confirm these drugs' safety and effectiveness in clinical settings for dual therapeutic uses, more in vivo research is advised.

References

1- Frumm SM, Fan ZP, Ross KN, et al. Selective HDAC1/HDAC2 inhibitors induce neuroblastoma differentiation. Chemistry & Biology. 2013 May 23;20(5):713-25. DOI: 10.1016/j.chembiol.2013.03.020

2- Kattar SD, Surdi LM, Zabierek A, et al. Parallel medicinal chemistry approaches to selective HDAC1/HDAC2 inhibitor (SHI-1:2) optimization. Bioorganic & Medicinal Chemistry Letters. 2009 Feb 15;19(4):1168-72. DOI: 10.1016/j.bmcl.2008.12.083

3- Methot JL, Hoffman DM, Witter DJ, et al. Delayed and prolonged histone hyperacetylation with a selective HDAC1/HDAC2 inhibitor. ACS Medicinal Chemistry Letters. 2014 Apr 10;5(4):340-5. DOI: 10.1021/ml500019u

4- Kazantsev AG, Thompson LM. Therapeutic application of histone deacetylase inhibitors for central nervous system disorders. Nature Reviews Drug Discovery. 2008 Oct;7(10):854-68. DOI: 10.1038/nrd2681

5- Tang Y, Lin YH, Ni HY, et al. Inhibiting Histone Deacetylase 2 (HDAC2) Promotes Functional Recovery from Stroke. Journal of the American Heart Association. 2017 Oct 5;6(10): e007236. DOI: 10.1161/JAHA.117.007236

6- Wagner FF, Zhang YL, Fass DM, et al. Kinetically selective inhibitors of histone deacetylase 2 (HDAC2) as cognition enhancers. Chemical Science. 2015;6(1):804-15. DOI: 10.1039/C4SC02721A

7- Sada N, Fujita Y, Mizuta N, et al. Inhibition of HDAC increases BDNF expression and promotes neuronal rewiring and functional recovery after brain injury. Cell Death & Disease. 2020 Aug 18;11(8):655. DOI: 10.1038/s41419-020-02875-1

8- Schroeder FA, Lewis MC, Fass DM, et al. A selective HDAC 1/2 inhibitor modulates chromatin and gene expression in brain and alters mouse behavior in two mood-related tests. PloS One. 2013 Aug 14;8(8):e71323. DOI: 10.1371/journal.pone.0071323

9- Mohseni J, Zabidi-Hussin ZA, Sasongko TH. Histone deacetylase inhibitors as potential treatment for spinal muscular atrophy. Genetics and Molecular Biology. 2013; 36:299-307. DOI: 10.1590/S1415-47572013000300002

10- Andreassi C, Angelozzi C, Tiziano FD, et al. Phenylbutyrate increases SMN expression in vitro: relevance for treatment of spinal muscular atrophy. European Journal of Human Genetics. 2004 Jan;12(1):59-65. DOI: 10.1038/sj.ejhg.5201080

11- Kim C, Choi H, Jung ES, et al. HDAC6 inhibitor blocks amyloid beta-induced impairment of mitochondrial transport in hippocampal neurons. PLoS One. 2012;7(8):e42983. DOI: 10.1371/journal.pone.0042983

12- Kontopoulos E, Parvin JD, Feany MB. α-synuclein acts in the nucleus to inhibit histone acetylation and promote neurotoxicity. Human Molecular Genetics. 2006 Oct 15;15(20):3012-23. DOI: 10.1093/hmg/ddl243

13- Dompierre JP, Godin JD, Charrin BC, et al. Histone deacetylase 6 inhibition compensates for the transport deficit in Huntington's disease by increasing tubulin acetylation. Journal of Neuroscience. 2007 Mar 28;27(13):3571-83. DOI: 10.1523/JNEUROSCI.0037-07.2007

14- Mahdi MF, Raauf AM. Molecular modelling, Synthesis and Antiproliferative Evaluation of New Phenyldiazenyl)-Pyrazol Schiff Base Derivatives. Al Mustansiriyah Journal of Pharmaceutical Sciences. 2024 Jan 14;24(1):25-37.
15- Jabbar ZA, Mahdi MF, Abd Razik BM. Synthesis, Characterization, ADME Study and Anti-proliferative evaluation against MCF-7 breast cancer cell line of new analog of a 4-aminophenyl quinazolinone derivative. Al Mustansiriyah Journal of Pharmaceutical Sciences. 2023 Oct 9;23(4):411-28.
16- Raauf AMR, Omar TN, Mahdi MF, Fadhil HR. Synthesis, molecular docking and anti-inflammatory evaluation of new trisubstituted pyrazoline derivatives bearing benzenesulfonamide moiety. Nat Prod Res. 2024 Jan-Feb;38(2):253-260. doi: 10.1080/14786419.2022.2117174.
17- Razik, B. M. A., Ezzat, M. O., & Al-Shohani, A. D. H. MOLECULAR DOCKING AND DESIGN STUDY FOR ANTICANCER ACTIVITY OF FLAVONOID DERIVATIVES AGAINST BREAST CANCER. INDIAN DRUGS, 57(04), 7–14(2020). https://doi.org/10.53879/id.57.04.12202.
18- M. Mohammed and A. Amjed Adnan, "In-silico design, molecular docking, molecular dynamic simulations, Molecular mechanics with generalised Born and surface area solvation study, and pharmacokinetic prediction of novel diclofenac as anti-inflammatory compounds", Turkish Comp Theo Chem (TC&TC), vol. 8, no. 3, pp. 108–121, 2024, doi: 10.33435/tcandtc.1355772.
19- Chennai HY, Belaidi S, Bourougaa L, Ouassaf M, Sinha L, Samadi A, et al. Identification of Potent Acetylcholinesterase Inhibitors as New Candidates for Alzheimer Disease via Virtual Screening, Molecular Docking, Dynamic Simulation, and Molecular Mechanics–Poisson–Boltzmann Surface Area Calculations. Molecules. 2024;29(6):1232. DOI: https://doi.org/10.3390/molecules29061232.
20- Agrawal K, Patel T, Thakur S, Patel K, Mittal S. Spectral Investigations, DFT Studies, ADME Analysis, Molecular Docking of New Piperidine Derivatives with Potential Antimicrobial Activity. J. Sci. Technol. 2023;16(35):2835-2844. DOI: https://doi.org/10.17485/IJST/v16i35.389.